Egyptian Journal of Soil Science
http://ejss.journals.ekb.eg/

Morphogenetic and Chemical Properties of Soils in the Receded Aral Sea Under Unsuitable Conditions for Cultivation

Zafarjon Jabbarov[1*], Tokhtasin Abdrakhmanov[1], Kholisa Eshova[1], Urol Nomozov[2], Shokhrukh Abdullaev[1], Elmurod Yangiboyev[1], Dilafruz Makhkamova[1], Otamurod Imomov[1], Nurmukhammad Zafarjonov[1], Boguslaw Wilkomirski[3] and **Saidjon Sidikov[1]**

[1]*National University of Uzbekistan, Tashkent, 100174, Uzbekistan*
[2]*Tashkent branch of the Samarkand state university veterinary medicine of livestock and biotechnologies, Chilanzar, 35a, Uzbekistan*
[3]*University of Warsaw, Faculty of Biology, Biological and Chemical Research Centre, Zwirki i Wigury 101, 02-089 Warsaw, Poland*

THE ARTICLE provides information on the formation and modification of soils in the area left behind by the drying of the Aral Sea, located in Central Asia. The research was conducted by dividing the region into three zones: Region I: the shores of the Aral Sea that dried up 50 years ago, Region II: sand deposits carried by wind, Region III: the central part that dried up 18-20 years ago. According to the results, Arenosols have formed in Regions I and II, while Solonchaks have developed in Region III. Over time, the properties of these soils have undergone various changes. For example, the humus content in the soils of Regions I and II has increased, reaching 0.14-0.47%, while in Region III, it has been recorded at 0.26%. The amount of available phosphorus in the soils of Region III was 13.40 mg/kg, whereas it ranged from 0.15 to 18.61 mg/kg in the soils of Regions I and II. Potassium content in the soils of Regions III was 86.01 mg/kg, compared to 72.45-136.52 mg/kg in Regions I and II. The degree of salinity also varied, increasing from Regions I to Regions III.
Based on the granulometric composition of the soils, the amount of physical clay (particles sized 0.01-0.001 mm) varies across the profiles. A tendency for an increase in the amount of physical clay (0.01-0.001 mm particles) was observed moving from Regions I to Regions III. The granulometric composition ranged from light loam to loose sand. This indicates that soil formation and transformation are most active in the regions with initially dried and wind-deposited sands, whereas in the central part, which dried more recently, soil transformation occurs at a slower pace.

Keywords: Soil, Aral Sea, salinity, humus sand, nutrients, organic matter, transformation, granulometric composition.

1. Introduction

The Aral Sea, located in the deserts of Central Asia, has been drained and saturated several times over the past 10,000 years (Micklin, 2007), the last drying up of the Aral Sea, located in Central Asia, began in 1960, and to date, 10% of its water has been preserved, and sands have appeared on a total area of 5.2 million hectares (Yanan Su et al, 2021, Jabbarov et al., 2024, Micklin, 2016), the drying up of the Aral Sea is one of the largest man-made ecological disasters in the world (Tony Waltham et al., 2002), The main reason for the subsequent drying up of the Aral Sea is the rapid development of irrigation (Micklin, 2010, Breckle et., 2012), 90% of the Aral Sea has dried up, scientific research is underway to restore it (He et al., 2022), however, the proposals of some scientists, including the supply of water from the Siberian rivers and the Caspian Sea, are at high risk of filling the Aral Sea with other major environmental problems (Badescu et al., 2010), so this is impossible (Aslanov et al., 2024, Jabbarov et al., 2025).

The drying up of the Aral Sea has been studied in many ways, with climate change being the main driving force behind the regression and transgression of the Aral Sea, while other scientists point to anthropogenic impacts as the main cause of changes in the water level of the Aral Sea relative to the Holocene (Cretaux et al., 2013). It has been proven that the drying up of the Aral Sea is caused by a high level of water consumption in agriculture, which has a greater impact than climate change (Aus der Beek et al., 2011), In the sands formed as a result of the drying up of the Aral Sea in the southern, eastern, western, and central regions, physical, chemical, and biological processes differed from each other (Izhitskiy et al., 2016). In the northern part of the Aral Sea, water changes during the growing season have a significant positive correlation with temperature (P=0.52) and a slight negative correlation with precipitation (P=-0.22), while in the western and eastern parts, on the contrary, there is

*Corresponding author e-mail: zafarjonjabbarov@gmail.com
Received: 16/09/2025; Accepted: 13/11/2025
DOI: 10.21608/ejss.2025.424117.2368

a significant negative correlation with temperature (P=-0.71 and -0.62) and precipitation (P=0.71 and 0.55) during the growing season (Berdimbetov et al., 2024). Due to the excessive use of water in agriculture from the Amu Darya and Syr Darya rivers, which flow into the Aral Sea, the Aral Sea has been drying up (Rufin et al., 2022), in 2000 and 2008, there was a serious water shortage in the Amu Darya delta, and very little water reached the Aral Sea (Jiang et al., 2020). Currently, the Aral Basin has a very complex system of canals, reservoirs, irrigated fields and hydraulic structures, including 7.9 million hectares (Orlovsky et al., 2021).

The drying up of the Aral Sea was influenced by rising temperatures, decreasing humidity, and precipitation, causing environmental problems (Loodin et al., 2020), resulting in the dried-up Aral Sea becoming a hotbed of salt-sand storms, especially in its northeastern part, and causing significant damage to the region (Indoitu et al., 2015). The drying up of the Aral Sea has created serious environmental problems for the countries of Central Asia, including the Republics of Uzbekistan and Kazakhstan (Jabbarov et al., 2025, Jabborova et al., 2023). As a result of the drying up of the Aral Sea, saline sandy soils began to form on its bottom (Ismanov et al., 2024). As a result of the drying up of the Aral Sea, sands appeared on large areas and salinization was observed due to strong evaporation (Gaeun et al., 2024), as a result of the drying up of the Aral Sea, sandy and clay soils appeared in its southeastern part, and as a result of the abundance of carbonates in them, worms appeared (Stulina et al., 2020).

In the sandy soils formed as a result of the drying up of the Aral Sea, salinization occurs, and salts are found in the 0-100 cm layer, with the largest amount of salts located in the 0-5 cm layer (Duan et al., 2022). As a result of the drying up of the Aral Sea, the Aralkum was formed on 2.6 million hectares, and bushes, saxauls, and halophytes were observed in these areas (Issanova et al., 2023), The main soils common in the Aralkum Desert, which arose on the replacement of the Aral Sea, are saline soils, which are composed of sands and solonchaks (Issanova et al., 2022, Jabbarov et al., 2024), and microorganisms (*Fusibacter, Halanaerobium, Guyparkeria, Marinobacter, Idiomarina, and Thiomicrospira)* have been found in the soil soils of the dried-up bottom of the Aral Sea, indicating soil formation in these areas (Chernyh et al., 2024). As a result of the drying up of the Aral Sea, the concentration of salts increased and remained in the muddy layer, causing soil salinization, in which *microorganisms Arthrobacter, Bacillus, Massilia, Rhodococcus and Nocardiopsis* were found (Šimonovičová et al., 2024). All soil-grounds formed on the dried-up bottom of the Aral Sea have undergone degradation, with a high degree of salinization and erosion (Kattayeva et al., 2022), and as a result of the Aral Sea's desiccation, bare hydromorphic solonchaks have developed on the newly exposed seabed. These soils are characterized by high surface salinity and a groundwater table located at a depth of less than 2 meters, which exerts a strong influence on their moisture and salt regime (Idirisov et al., 2023).

2. Materials and Methods

2.1. Study area

2.1.1. Localization and climate

The study area is located in the eastern part of the former Aral Sea, encompassing an area of over 900 km² (Zonn et al., 2009). This region is characterized by a continental climate, which is defined by cold winters and hot summers. In the aftermath of the sea's disappearance, the eastern Aral Sea basin now experiences a severe desert climate, characterized by minimal annual rainfall, extremely high summer temperatures, and harsh winter conditions (Berdimbetov et al., 2021). The significant reduction in water surface area has resulted in decreased humidity, thereby exacerbating temperature extremes. The average annual air temperature is recorded at 12.7°C, while mean annual precipitation is approximately 105 mm. Peak temperatures occur in July, averaging 36.1°C, whereas January experiences the lowest temperatures, averaging −11.0°C. Summer precipitation is notably sparse, remaining below 3 mm per month, with levels falling below 1 mm in August and September. In contrast, late winter to early spring (February-March) sees an increase in precipitation, rising to 22-25 mm per month (Huang et al., 2022; Micklin and Aladin, 2008). The environmental degradation and distinctive climate changes in the eastern Aral Sea region underscore the urgent necessity for sustainable practices to address the socio-environmental challenges associated with these conditions.

2.1.2. Hydrological Evolution Phases of the Aral Sea Basin

Water resources in Central Asia were distributed differently over time, and the Aral Sea dried up in the 15th century BC, 1211 BC, and the present day, while the remaining periods were characterized by high, low, and average water levels. The current drying up of the Aral Sea is not the first, it has already dried up several times before, and the water level has decreased. There is no clear tendency or regular time for its drying up or filling, according to available data, the Aral Sea dried up in the 15th century BC, 1000 years later, in the 5th century BC, there was water again, after 200 years, that is, in the 3rd century BC, there was water. Another 200 years passed, and the water of the Syr Darya, which flowed into the Aral Sea, sharply decreased, from which it existed until the 10th century, and by 1211 the Aral Sea had again dried up. Over time, the water increased in 1320 and 1375,

in 1400 the water in the Aral Sea again sharply decreased, in 1575 it was full again, in 1638 the amount of water decreased again, by 1680 the water increased again, by 1868 the Aral Sea was full, in 1960 the Aral Sea was full, by 2000 the water was at a low level, by 2024 the Aral Sea had almost dried up and 10% of its water remained (Duxovny, 2017). According to the available paleogeographical and hydrological data, the history of the Aral Sea shows repeated cycles of desiccation and refilling that occurred over several millennia. However, determining exact dates for these events remains challenging due to limited and sometimes inconsistent historical evidence. Previous interpretations suggesting that the sea dried up in the 15th century BC, 1211 BC, and in the present era are now considered approximate rather than definitive. The cited sources (Cretaux et al., 2013; Dukhovny, 2017) describe general Holocene fluctuations in the Aral Sea's level, but they do not provide such specific chronological points. More accurately, these fluctuations can be viewed as recurring hydrological phases within the last 3,500 years, characterized by alternating periods of expansion and regression (Table 1).

Table 1. Historical Accounts of the Aral Sea's Hydrological System.

Periods	Status of the Aral Sea	Time difference, in a year	Duplicate build time, in a year	Recurrence of the water level drop period	Payback period, in a year
B.c.15th century	Dry				
B.c.5th century	Available	1000			
B.c.3rd century	Full of With water	200			1200
Year 1211	Nearly Dry	1400	2600		
Year 1320	Middle level	109			
Year 1375	Available	55			
Year 1400	Low level	25		25	
Year 1575	High level	175			1800
Year 1638	Low level	63		238	
Year 1680	Available	42			
Year 1858	High level	178			220
Year 1960	Full of With water	102			
Year 2000	Low level	40		320	
Year 2024	Nearly dry	24	704		

Only the time between the drying up and filling of the Aral Sea varies, according to the analysis, after 1000 years after the initial drying up, the Aral Sea was filled up again, and after 400 years it dried up again, and after 704 years, the Aral Sea dried up again for a third time, and over time, as a result of the drying up and filling of the sea water, 5.2 million hectares of different soils formed and various plant species grew.

These studies were conducted in 2024, soil sections were dug and soil samples were taken in the eastern part of the dried-up bottom of the Aral Sea. The drying process of the Aral Sea began in 1960 precisely from the eastern part of the region, and soil profiles were conducted to study soil profiles in the dried-up area 20 and 30 years after the initial dried-up points. That is, a comparative comparison was conducted with the area where water first withdrew and soil formation began, followed by a comparison of the soils of the dried-up areas, a comparison of changes in the morphological characteristics of the soil, and a study of differences in the distribution of the plant world in the area.

Throughout its history, the Aral Sea has experienced fluctuations of varying magnitude, with water levels alternating between dry, low, medium, and high stages. According to paleogeographic interpretations, these phases occurred approximately 2,700-3,500 years ago; however, it was not possible to measure the water volume and surface elevation with precision during those times. Therefore, these data should be regarded as approximate rather than exact. To provide a generalized understanding of these hydrological transitions, researchers have used a conditional 100-point scale to describe the relative states of the sea: the completely dry stage was assigned 0 points, the nearly dry stage 10-20 points, the low-water stage 40 points, and the medium-level stage 50 points. This scale serves as a comparative framework to characterize historical changes in the Aral Sea's condition rather than as an exact quantitative measurement. Based on which the condition of the Aral Sea was assessed for the first time on a 100-point scale, according to which the dry period was assessed as 0; the almost dry period - 10-20; the period of low level - 40; the period of medium level - 50; the existing period (Fig. 1).

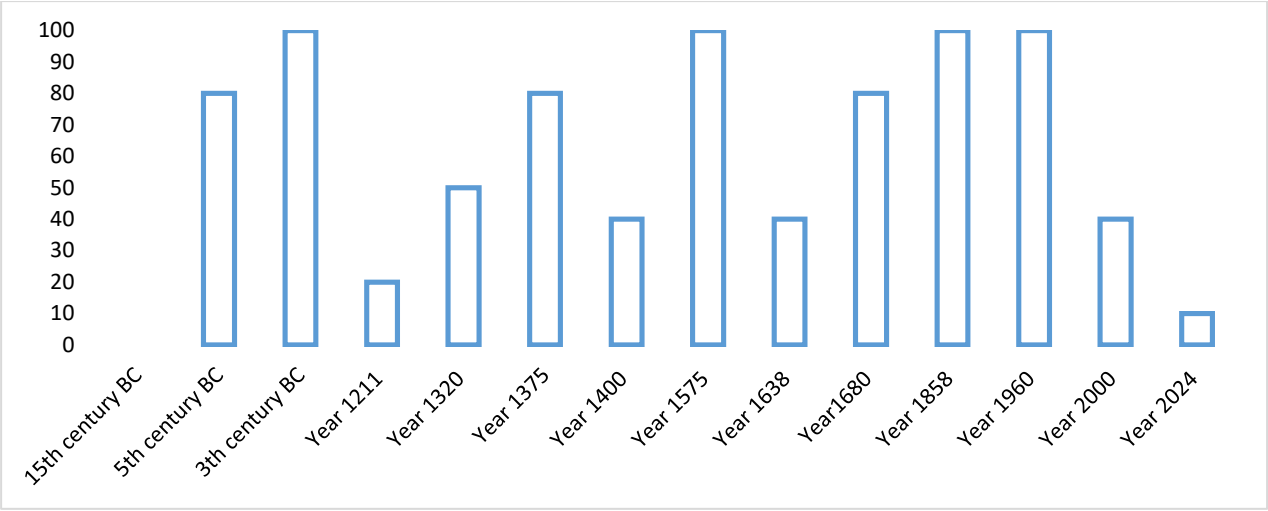

Fig. 1. Dynamics of the historical change in the drying and filling of the Aral Sea on a 100-point scale, %.

Although genetic layers were not formed in the formation of soils on the dried-up bottom of the Aral Sea, soil formation processes occurred over many years and soil layers were formed. As a result of being submerged for many years and drying up again, various morphological features, chemical and physical properties were formed.

2.1.3. Geology and parent materials for soils

The eastern side of the former Aral Sea, primarily situated in Uzbekistan and extending into Kazakhstan, presents a distinctive geological configuration that significantly influences soil formation and composition (Micklin and Williams, 2019; Peter, 2005). The geology of this region encompasses several critical characteristics. Specifically, the Aral Sea basin, particularly its eastern sector, is characterized by extensive sedimentary deposits resulting from the retreat of the sea. These deposits are predominantly composed of alluvial (river-borne) and lacustrine (lake-bed) sediments, which include sands, silts, and clays. Notably, these sediments often exhibit saline and alkaline properties due to the high concentrations of salts left behind by the receding Aral Sea, which in turn affects soil chemistry and plant growth(Aslanov et al., 2024; Opp et al., 2024). The Amu Darya and Syr Darya rivers, which historically nourished the Aral Sea, deposited substantial amounts of sediment in the delta regions. These sediments are rich in alluvium materials transported by flowing water and encompass a mixture of fine particles, including clay, silt, and sand. Over time, the shrinking of the sea has exposed these deltaic deposits, thereby influencing the texture and nutrient profile of the soils in the area(Christian et al., 2019). Additionally, wind activity within the Aral Sea basin, particularly following the sea's retraction, has facilitated the accumulation of eolian deposits. This phenomenon has contributed to the formation of sandy soils, which are particularly susceptible to erosion and salinization. The prevailing arid conditions and the scarcity of vegetation exacerbate these effects. Many of the soils on the eastern side exhibit high salinity and commonly contain gypsum and other evaporite minerals, especially in regions proximal to the former shoreline. Overall, the soils on the eastern side of the former Aral Sea are profoundly shaped by the region's geological history, with alluvial, lacustrine, and eolian deposits influencing their texture, salinity, and mineral composition. The elevated levels of salts, gypsum, and sandy textures pose significant challenges for both vegetation and agricultural endeavors (Duan et al., 2022).

2.1.4. Geomorphological context

The geomorphological context of the eastern side of the former Aral Sea is shaped by a confluence of ancient fluvial activity, extensive aridification, and the dramatic regression of the sea itself. These processes have resulted in a distinctive landscape characterized by varied landforms and challenging environmental conditions(Indoitu et al., 2015). The plains are primarily composed of sandy and silty deposits, which were deposited by ancient rivers and aeolian processes. The lowlands are predominantly flat, interspersed with occasional undulating dunes and sparse vegetation, which reflect the region’s desert-like climate and limited water availability. Historically, the deltas of the Amu Darya and Syr Darya rivers are significant features in the geomorphology of the area. These deltas previously contributed substantial quantities of sediment to the Aral Sea, fostering extensive wetland and riparian regions(Khaydar et al., 2021). With the shrinkage of the Aral Sea, much of the former delta region has now become arid, revealing channels, levees, and floodplains that are severed from regular water flows. Overall, the geomorphological landscape of the eastern side of the former Aral Sea illustrates a transition from once-fertile deltas and wetland ecosystems to desertified plains and salt flats. This transformation is driven by a combination of natural geomorphological processes and significant

anthropogenic impacts resulting from water diversion, which has led to the near disappearance of the Aral Sea (Alikhanova and Bull, 2023).

2.2. Selection of research points and soil sampling

2.2.1. Selection of research points

The dried-up bottom of the Aral Sea currently covers an area of 5.2 million hectares, featuring various types of soils and substrates. To identify distinct differences in soil transformation, three regions were selected as research sites: Region I: initially dried area (Profiles 1 and 2), Region II: sands deposited by wind (Profiles 3 and 4), Region III: area near the center of the Aral Sea (Profile 5). The study compared the soils of these three regions, highlighting differences in their chemical and physical properties. This approach provided an opportunity to analyze and compare the characteristics of soils across these regions.

2.2.2. Soil sampling

Soil samples were collected from the three regions mentioned above. Their coordinates, formation conditions, and classification names according to the WRB are provided in Table 2 below.

Table 2. Soil profile location regions and classification (in the eastern part of the dried-up Aral Sea).

Study region (eastern part)	Profile	Coordinates	Soil formation state	According to the WRB. (2022) classification
Dry Aral Sea coastline (Region I)	1- Profile	N43°41′81.57″ E60°18′10.42″	weakly developed sandy soils formed on aeolian deposits	Arenasols
	2- Profile	N43°43′74.09″ E60°17′93.05″		Arenasols
Aeolian sands of the Aral Sea bed (Region II)	3- Profile	N43°67′43.37″ E60°17′17.23″	weakly developed sandy soils formed from wind-blown (aeolian) deposits	Arenasols
	4- Profile.	N43°82′89.45″ E60°19′95.43″		Arenasols
Aeolian sands of the Aral Sea bed (Region III)	5- Profile	N43°93′26.33″ E60°25′45.61″	Calcium carbonate rich soils with low to moderate salinity formed under arid conditions	Solonchaks

Various factors were considered when collecting soil samples from the dried-up bottom of the Aral Sea. It was essential to take samples from designated geographic points, representing different areas of the dried-up bottom and various soil types (Fig 2).

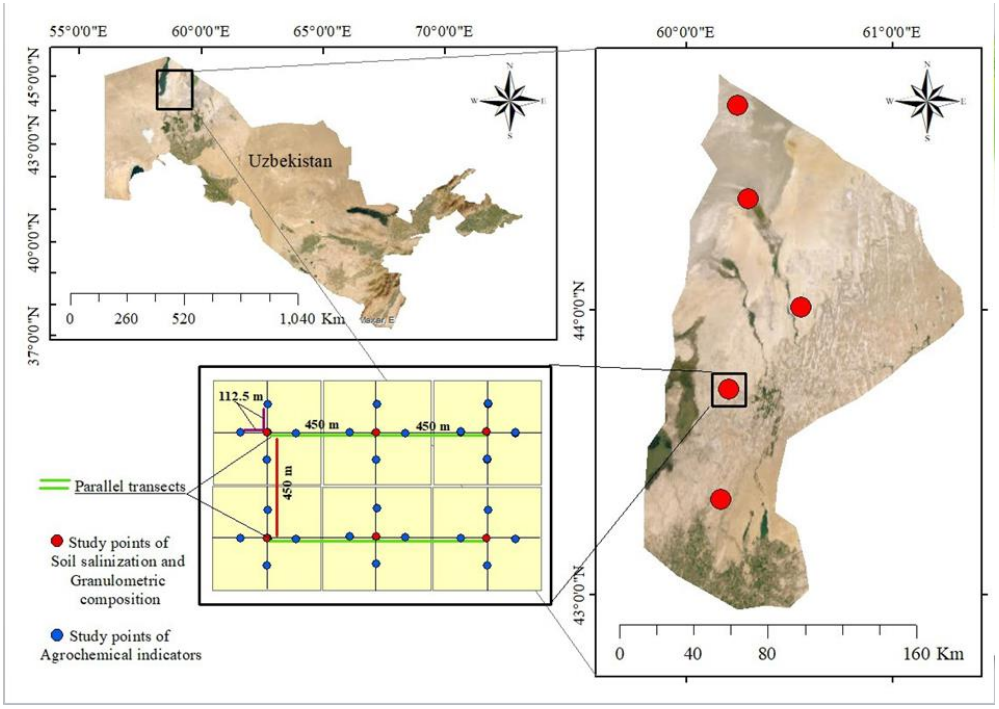

Fig. 2. Study area and soil profiles location.

These samples were intended to determine the salt content, chemical composition, and other properties of the soils.

2.2.3. Formation of soil morphological characteristics

Looking at the historical process of the Aral Sea, it has dried up and refilled several times over the past ten thousand years. During the dry periods, soils formed to some extent but were subsequently buried under sands and salts. The accumulation of mud layers, aquatic plants, and animal remains under water led to the formation of organic matter, facilitating humus development. The deposition of new sands over these newly formed soils altered their genetic horizons. This means that the usual soil formation patterns observed in plains or mountainous areas were not seen on the dried-up bottom of the Aral Sea. The morphological characteristics of the collected soil profiles can be described as follows:

Profile 1: Arenasols - weakly developed sandy soils formed on aeolian deposits (Fig. 3). The area is located in the eastern part of the Aral Sea, where the *Halochylon ammodendron* (C.A.Mey.) *Bunge ex Fenzl and Alhagi pseudalhagi* (M.Bieb.) Desv. ex Wangerin plants dominated, the soil consisted of uneven sands, located on sandy deposits, and the upper part was slightly crusted.

0-14 cm. Light gray, sandy in mechanical composition, salts are indistinguishable to the eye, the layer is dry without moisture, non-dense, has a dusty structure, shells are very small, visible only sporadically, plant roots and insect traces are common, moving to the next layer with a change in moisture content.

14-33 cm. Light gray, sandy and sandy in mechanical composition, salts are indistinguishable to the eye, moderately moist, slightly compacted, has a dusty structure, shells are very rare, plant roots and insect traces are common, passing to the next layer with increased moisture and a change in color.

33-48 cm. Light brown, light loam and sandy loam in mechanical composition, white plaster crystalline spots are found in the layer, moderately moistened, highly compacted, has a layered and clumpy structure, stains of rust are rare, plant roots and insect traces are rare, transitioning to the next layer with a change in mechanical composition.

48-77 cm. Light brown, medium loam mechanical composition, heavy mechanical composition soils-grounds are also found in the layer, white gypsum crystalline spots are rare, moderately moistened, moderately dense, has a layered structure, rust spots are common, plant roots and insect traces are rare, transitioning to the next layer with a change in color.

77-83 cm. It is grayish-yellow in color, the mechanical composition is not sandy, salts are absent, the moisture content is very high, it is not compacted, the roots of the plant are rarely found, insect traces are not found, and it transitions to the next layer with a change in its mechanical composition.

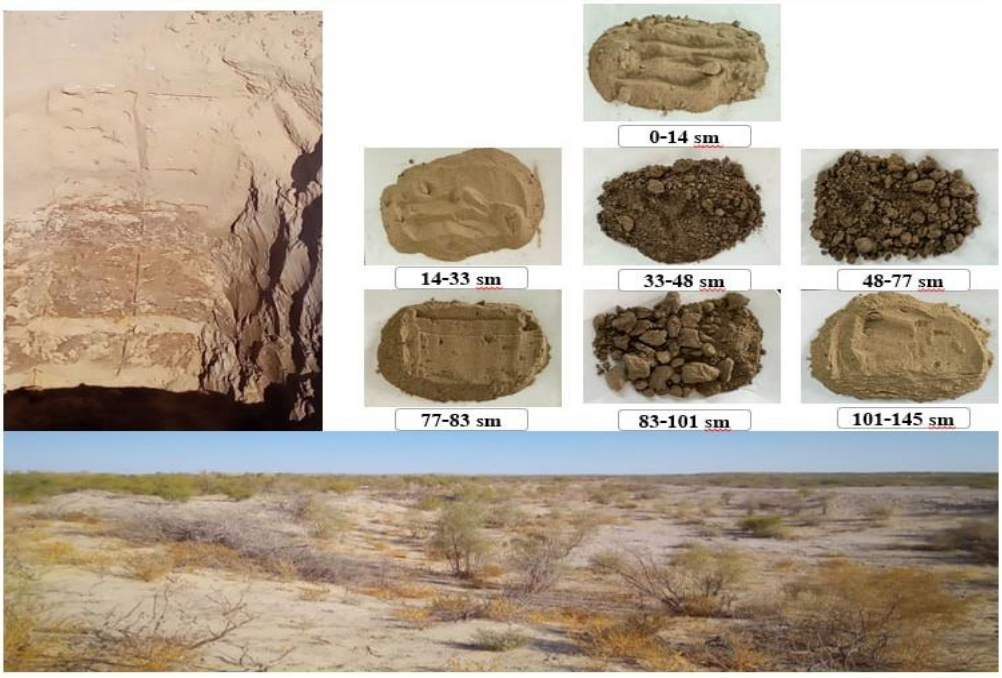

Fig. 3. Morphological characteristics of soil samples and profile 1 of the dried-up bottom of the Aral Sea.

83-101 cm. It is grayish-yellow in field color, medium loamy in mechanical composition, moderately moistened, moderately compacted, has a layered structure, rarely presents rust spots, the roots of the plant are sparse, insect traces are absent, and then transitions to the horizon with a change in mechanical composition.

101-145 cm. It is grayish-yellow in field color, sandy in mechanical composition, moderately moist, poorly compacted, often contains rust spots, the roots of the plant are sparse, no traces of insects are found, then it transitions to the next layer with a change in mechanical composition.

Profile 2. Arenasols - weakly developed sandy soils formed on aeolian deposits (Fig. 4). The eastern part of the Aral Sea, where *Halostachys caspica* (M.Bieb.) C.A. Mey predominates, the soil is covered with bark, moisture is noticeable, and a layer of bark is present on the upper part, resembling a strong crust.

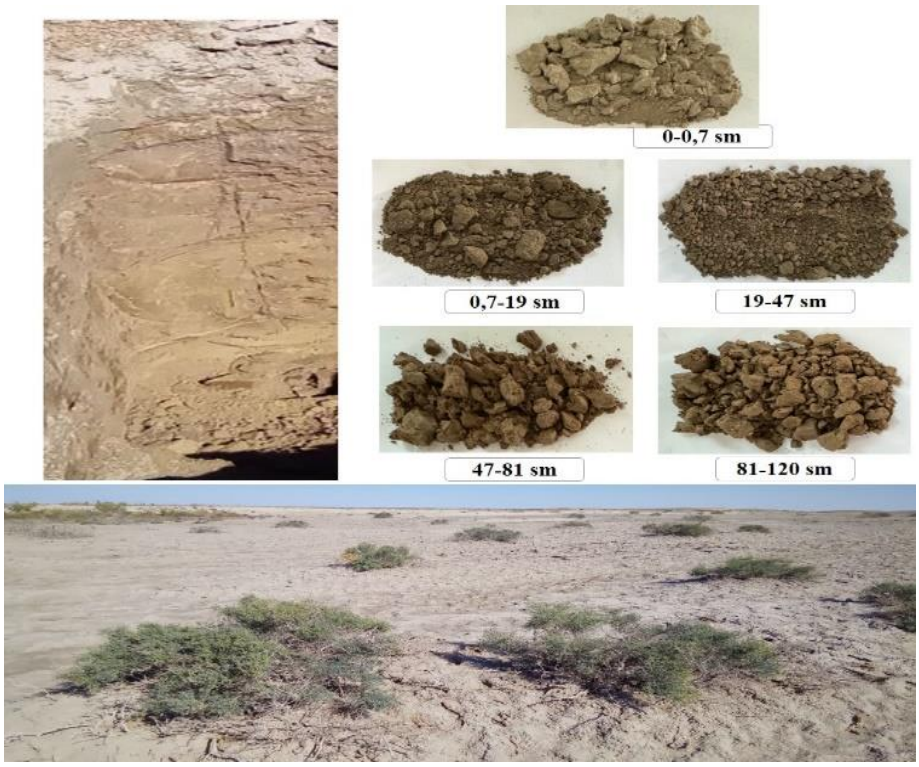

Fig. 4. Morphological characteristics of profile 2 and soil samples on the dried-up bottom of the Aral Sea.

0-0.7 cm. Coated, light gray, light loam in mechanical composition, dry unmoistened, shells are rare, have a dusty structure, do not compact.

0.7-19 cm. Gray-brown in color, heavy loam in mechanical composition, medium loam in the layer, moderately moistened, has a layered and cloddy structure, white gypsum crystalline spots are found in the layer, stains of rust are rare, plant roots and insect traces are rare, then transition to the layer with a change in color.

19-47 cm. Light brown, heavy loam in mechanical composition, soils of medium mechanical composition are also found in the horizon, white gypsum crystalline spots are rare, moderately moistened, moderately dense, has a layered structure, rust spots are common, plant roots are rarely traced by insects, then transition to the horizon with a change in color.

47-81 cm. Light brown, medium loamy in mechanical composition, moderately moistened, moderately compacted, with a layered structure, rare rust spots, sparse plant roots, no insect traces, then transitioning to a layer with a change in mechanical composition.

81-120 cm. Light brown in color, light loamy in mechanical composition, moderately moistened, poorly compacted, has a dusty and layered structure, stains of rust are rare, plant roots are sparse, no insect traces are found.

Profile 3. Arenasols - weakly developed sandy soils formed from wind-blown (aeolian) deposits (Fig. 5). The eastern part of the Aral Sea, with sparse vegetation in the area, is represented by the *Halochylon ammodendron* (C.A. Mey.) The plant Bunge ex Fenzl dominates, shells are found above ground, there is a thin black layer in the aboveground part, the aboveground mezor relief consists of low elevations, and volatile sands.

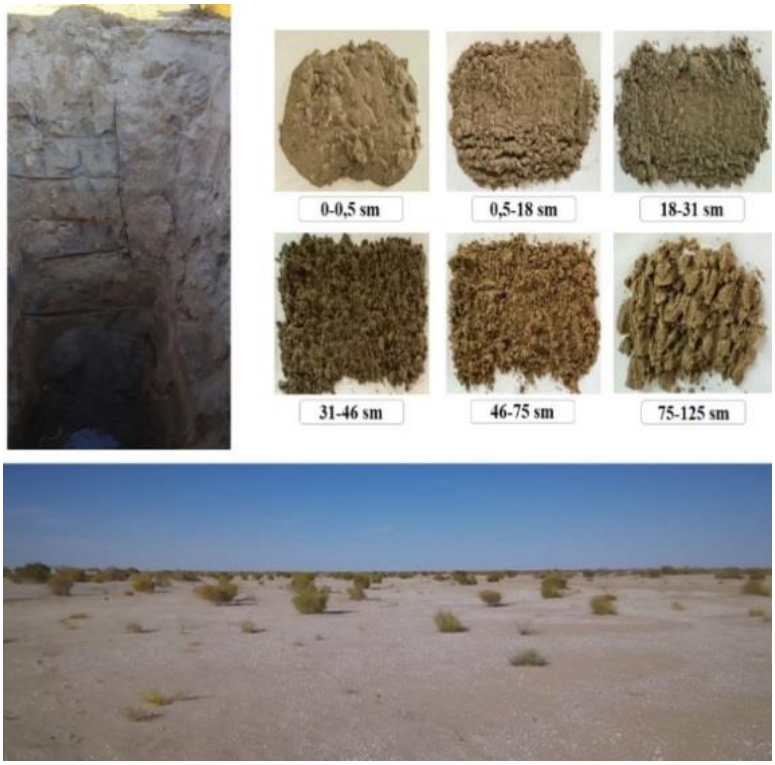

Fig. 5. Morphological features of profile 3 and soil samples on the dried-up bottom of the Aral Sea.

0-0.5 cm. Coated, light gray, sandy and sandy in mechanical composition, dry, unmoistened, shells are common, have a dusty structure, plant roots are common, not compacted.

0.5-18 cm. Light gray, sandy and sandy in mechanical composition, unmoistened dry, shells are common, non-dense, has a dusty structure, stains of rust are rare, plant roots and insect traces are common, significantly transitioning to the next layer with a change in color and increased moisture content.

18-31 cm. Gray, sandy and sandy in mechanical composition, moderately moistened, shells are rare, non-dense, have a dusty structure, stains of rust are rare, plant roots and insect traces are rare, root residues are rare, slowly transitioning to the next layer with a change in color.

31-46 cm. Light gray, sandy and sandy in mechanical composition, moderately moist, shells are rare, non-dense, have a dusty structure, stains of rust are rare, plant roots and insect traces are rare, root residues are rare, slowly transitioning to the next layer with increasing stains of rust.

46-75 cm. Light gray, sandy and sandy in mechanical composition, moderately moist, shells are rare, non-dense, have a dusty structure, stains of rust are moderate, plant roots are rare, insect traces are not found, root residues are rare, passing to the next layer with a change in color.

46-75 cm. Light gray, sandy and sandy in mechanical composition, heavily moistened, shells are absent, non-dense, stains of rust are moderate, plant roots are rare, insect traces are absent, root residues are rare.

Profile 4. Arenasols - weakly developed sandy soils formed from wind-blown (aeolian) deposits (Fig. 6). Located in the eastern part of the dried-up bottom of the Aral Sea, the area has very little vegetation, *Haloxylon ammodendron* (C.A.Mey.) The plant Bunge ex Fenzl dominates, is located on marine deposits, shells are abundant on the surface, the surface is smooth, consisting of crustal crusts and dry sands.

Fig. 6. Morphological characteristics of soil samples and profile 4 on the dried-up bottom of the Aral Sea.

0-1 cm. It is coated, light gray in color, sandy and sandy in mechanical composition, dry, unmoistened, shells are very common, has a dusty structure, scattered, poorly attached, plant roots are found, not compacted.

1-25 cm. Light gray color, sandy and sandy in mechanical composition, low humidity, abundance of shells, non-dense, dusty structure, abundance of plant roots and insect traces, gradually transitioning to the next layer with increasing color, mechanical composition, and moisture content.

25-65 cm. Dark brown, heavy in mechanical composition, the loam horizon is berch clay, when excavating it turns out to be piecewise, it is difficult to dig with a shovel, heavily moistened, has a very strongly compacted, layered structure, rust spots are very common, plant roots and insect traces are rare, root residues are common, then slowly transitions into the horizon with a change in color.

65-115 cm. Dark blue, clay color, heavy loam in mechanical composition, heavy loam berch clay, strongly moistened moisture, very strongly compacted, has a layered structure, rust and bluish spots are very common, plant roots are rarely found, insect traces are not found, root residues are rare.

Profile 5. Solonchaks - Calcium carbonate rich soils with low to moderate salinity formed under arid conditions (Fig.7). The eastern part of the Aral Sea, with very little vegetation in the area, is represented by *Halocnemum strobilaceum (Pall.)* M. Bieb is dominated by plants, shells are abundant on the surface, the surface is smooth, consisting of crust-like crust, and dry sands.

Fig. 7. Morphological features of profile 5 and soil samples on the dried-up bottom of the Aral Sea.

0-0.8 cm. Coated, light gray, sandy and sandy in mechanical composition, dry, unmoistened, shells are very common, have a dusty structure, plant roots are common, not compacted.

0.8-24 cm. Light gray, sandy and sandy in mechanical composition, poorly moistened, shells are common, non-dense, have a dusty structure, scattered, poorly attached, plant roots and insect traces are common, moving to the next layer with increasing mechanical composition and moisture.

24-44 cm. Light brown, medium-loamy in mechanical composition, swampy and rusty, moderately moistened, moderately compacted, has a layered structure, rust spots are common, plant roots and insect traces are rare, root residues are rare, gradually transitioning to the next layer with a change in moisture content.

44-72 cm. Dark blue-clay-green color, mechanical composition is sandy, strongly moisture-like, slightly compacted, stains of rust and blueness are very common, plant roots are rare, insect traces are absent, root residues are rare, clearly transitioning to the next layer with a change in mechanical composition

72-138 cm. Dark blue-clay-green color, light loam mechanical composition, very strongly moistened clay layer, low density, stains of rust and blue are very common, plant roots are rare, insect traces are not found, root residues are rare.

2.4. Laboratory analysis methods

The determination of the physical and chemical properties of soils was conducted in accordance with internationally and regionally recognized analytical standards. The particle-size distribution (mechanical composition) of the soils was assessed using the sedimentation method as described in GOST 12536-2014, which provides a detailed classification of soil texture based on particle fractions. The content of organic matter and total carbon was determined following the GOST 26213-91 standard, applying the dichromate oxidation technique. The quantification of total nitrogen was carried out according to GOST 26107-84 using the Kjeldahl method, while total phosphorus was determined following GOST 26205-91, which involves extraction with an ammonium-lactate solution. Total potassium content was analyzed using GOST 26204-91 by means of flame photometry. These analytical procedures ensured the reliable quantitative assessment of the principal agrochemical elements within the studied soil samples.

2.5. Statistical analyses

The accuracy of laboratory analysis results and the impact of one or more factors on the variables were assessed and compared using the ANOVA (Analysis of Variance) method. The study analyzed the interaction of various factors in the soils of the research area, including: pH values in (H_2O) solutions, EC indicators (1:5 ratio) and their relationship to the total soluble salts, humus content, C:N ratio, and N results, the contribution of physical clay in the mechanical composition, and the interaction of total P and K content.

3. Results

3.1. Normality test

To ensure the reliability of the research results and their compliance with standards, a normality test (normal distribution) was conducted. The following results were obtained (Table 3).

Table 3. Normality test analysis of research results.

Variable\Test	Shapiro-Wilk	Anderson-Darling	Lilliefors	Jarque-Bera
pH_{H2O}	0,000	0,001	0,003	0,020
pH_{KCl}	<0,0001	<0,0001	0,000	0,011
$EC_{1:1}$	<0,0001	<0,0001	<0,0001	0,004
$EC_{1:5}$	<0,0001	<0,0001	<0,0001	0,001
Humus	0,003	0,032	0,193	0,076
C:N	0,004	0,002	0,006	0,642
N	<0,0001	<0,0001	<0,0001	0,002
P	0,004	0,010	0,002	0,123
K	0,003	0,005	0,018	0,097
K_2O	<0,0001	<0,0001	<0,0001	0,074
Physical clay sum	<0,0001	<0,0001	<0,0001	0,021

Since the calculated p-value was lower than the significance level of $\alpha = 0.05$, the null hypothesis (H_0) is rejected, and the alternative hypothesis (H_a) is accepted.

3.2. Soil salinity and electrical conductivity (EC), pH indicators

Electrical conductivity and pH environment of the soils formed in the dried-up bottom of the Aral Sea were found to vary. The results indicate that the profiles from the Aral Sea shores (Profiles 1 and 2), the sand dunes deposited by wind (Profiles 2 and 3), and the area near the central part (Profile 5) exhibited different results. For example, in Profile 1 from the Aral Sea shores, the pH in the 0-14 cm layer was 7.8, and in the 14-33 cm layer, it was 7.5. This indicates a gradual decrease in pH from mildly alkaline to neutral as we move deeper into the profile. In Profile 2, the pH of the upper 0-0.7 cm layer was 7.1, and in the subsequent layers, it was 6.7, 6.8, and 6.9 in the 0.7-19 cm, 19-47 cm, and 47-81 cm layers, respectively. In the 81-120 cm layer, the pH increased back to 7.1. This shows that the highest and lowest salinity levels were found in the top and bottom layers, respectively. Electrical conductivity (EC) values also varied. In Profile 1, the EC1:1 value decreased from 3.5 in the upper layers to 2.1 in the lower layers, while the EC1:5 value decreased from 3.7 to 2.3. In Profile 2, the EC1:1 and EC1:5 values were higher in the upper and lowest layers, with the intermediate layers showing lower values. These results suggest that the soils from Profiles 1 and 2 taken from the Aral Sea shores are weakly saline.

In soils formed from sands deposited by wind, the pH and EC values differ from those in the previously described soils. For example, in Profile 3, the pH in the 0-0.5 cm layer was 8.9, and it decreased gradually towards the lower layers, reaching 7.7 in the 75-125 cm layer. The EC values in the upper layers were 5.1 for EC1:1 and 5.3 for EC1:5, while in the lower 75-125 cm layer, they were 3.2 and 3.5, respectively. In Profile 4, a saline layer formed in the 0-1 cm layer, where the $pH_{(H2O)}$ was 9.2 and the $pH_{(KCl)}$ was 9.5. In the lower 65-125 cm layer, the $pH_{(H2O)}$ was 8.1 and the $pH_{(KCl)}$ was 8.5. The EC values were significantly higher in the upper 0-1 cm layer, with EC1:1 at 8.3 dS/m and EC1:5 at 8.6 dS/m. These values indicate high salt content in this layer, much higher than in other layers. In the lower 65-125 cm layer, the EC1:1 was 4.2 dS/m, and the EC1:5 was 4.5 dS/m. These results suggest that the soils in Region II, formed from wind-deposited sands and salts in the dried-up bottom of the Aral Sea, have higher pH and EC values in the upper layers due to the accumulation of transported salts.

In Region III, located near the central part of the dried-up bottom of the Aral Sea, the pH environment in Profile 5 showed the following characteristics: In the 0-0.8 cm layer, the $pH_{(H2O)}$ was 9.4, and the $pH_{(KCl)}$ was 9.7. The pH values decreased with depth, reaching $pH_{(H2O)}$ 7.9 and $pH_{(KCl)}$ 8.3 in the 72-138 cm layer. The EC values in these soils were also high in the upper 0-0.8 cm layer, with EC1:1 at 8.6 dS/m and EC1:5 at 8.9 dS/m. In the lowest 72-138 cm layer, the EC values decreased significantly, with EC1:1 at 4.0 dS/m and EC1:5 at 4.3 dS/m. This indicates a reduction in salinity with increasing depth in this region.

Dissolved ions in water form the total dry residue and also directly affect the pH (H_2O) value and the electrical conductivity (EC) ratio (1:5) of the soil environment. The indicators of the samples were analyzed using the Analysis of Variance for (pH_{H_2O}). The results showed that there were no significant differences between the groups (Pr > T) at the (0.0001***) level (Table 4).

Table 4. Analysis of $pH_{(H_2O)}$ and $EC_{1:5}$ values of soil samples through Pr > T between groups.

Source	Value	Standard error	t	Pr > |t|	Lower bound (95%)	Upper bound (95%)	p-values signification codes
pH_{H2O}	1,853	0,240	7,729	<0,0001	1,380	2,327	***
$EC_{1:5}$	-1,180	0,240	-4,921	<0,0001	-1,654	-0,707	***

Signification codes: 0 < *** < 0.001 < ** < 0.01 < * < 0.05 < . < 0.1 < ° < 1

In order to determine the differences between the analyses, the standard residual indicators for total dry residue were calculated. According to the results, in Profile 2 and Profile 4, most of the residuals were positive, while in Profile 1, there was a balanced distribution of positive and negative residuals. In Profile 3, the majority of the residuals were negative, while in Profile 5, most of the residuals were positive (Figure 8).

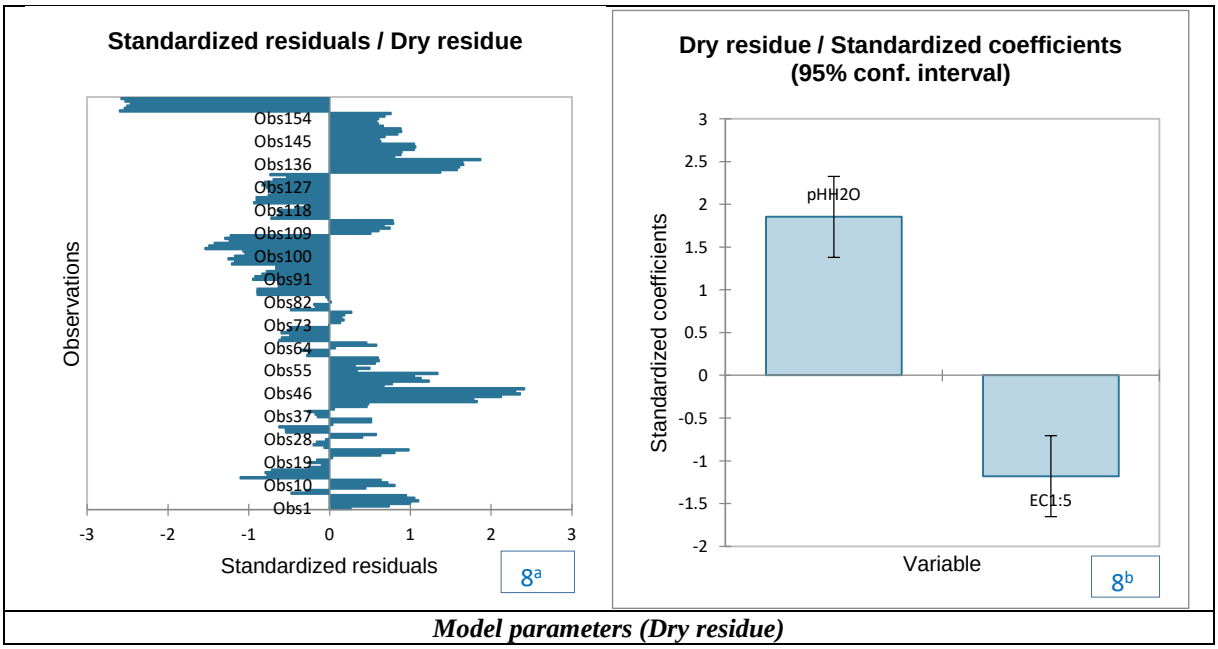

Fig. 8. Relationship between $pH_{(H_2O)}$ and $EC_{1:5}$ values and dry residue (Dry residue / Standardized coefficients, 95% confidence interval).

In Profiles 2 and 5, high values for the number of samples were observed, for example, obs 46-48 and obs 138-157 (Figure 8[a]). The standardized coefficients for the pH and EC relative to the total dry residue were 1.853 ± 0.240 and -1.180 ± 0.240, respectively (Figure 8[b]).

To analyze the results further and identify differences between groups, Linear Discriminant Analysis (LDA) was applied. According to the LDA results, Axis 1 corresponds to the ratio of pH_{H_2O} and $EC_{1:5}$, while Axis 2 is related to the dry residue. When the groups were plotted on these axes, the distribution of the samples across the profiles was as follows (Figure 9).

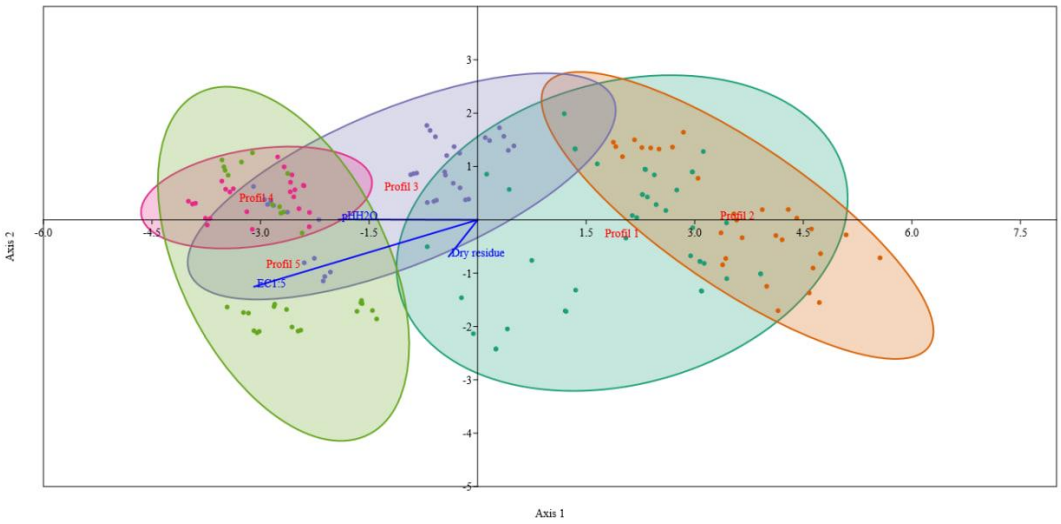

Fig. 9. Distribution of soil pH_{H2O}, $EC_{1:5}$ indicators, and dry residue in group samples through LDA (Linear Discriminant Analysis) analysis.

According to the analysis, the distribution of Profile 1 and Profile 3 samples along both axes is similar. The distribution of Profile 2 and Profile 5 samples along Axis 1 is also similar. In Profile 4, however, the distribution along Axis 1 is less spread compared to nearly all the samples in the other profiles. The results suggest that the formation of Profile 1 soils has been significantly faster compared to the other profiles, which is why the pH_{H_2O} and $EC_{1:5}$ values are not as high. The distribution of dry residue is less in Profile 1 layers because the amount of

cations and anions has decreased. The results from Profile 4 are closer to those of Profiles 3 and 5, mainly because they are located in areas with similar relief characteristics, suggesting a more uniform environment. For example, The granulometric and morphological characteristics of Profile 4 indicate that its properties closely resemble those of Profiles 3 and 5. All three profiles are located within low-lying, gently sloping relief zones of the desiccated Aral Sea basin, where aeolian sands dominate the surface sediments. In these areas, the accumulation of fine particles is minimal, and the physical texture remains predominantly sandy. The content of particles smaller than 0.01 mm ranges from 4% to 24.1% in Profile 3 and decreases to around 2% in Profiles 4 and 5. Such similarities in fine fraction distribution and geomorphological position explain why Profile 4 exhibits comparable granulometric composition and soil-forming dynamics to Profiles 3 and 5. These findings suggest that the formation of these profiles has been governed by similar environmental processes, including wind-driven sedimentation, high evaporation, and low groundwater influence.

3.3. Agrochemical Indicators

The section on agrochemical indicators has been revised to ensure consistency between zonal averages and profile-based data. The revised text now presents the results as averaged values for each region, supported by corresponding profile observations. The analysis shows that the agrochemical composition of soils varies noticeably across Regions I, II, and III of the dried Aral Sea bottom. The humus content in Regions I and II ranges from 0.14% to 0.47%, reflecting the sandy and sandy-loam texture of these soils, which contain relatively low organic matter. In Region III, the average humus content is 0.26%. Similarly, available phosphorus (P) ranges from 0.15 to 18.61 mg/kg in Regions I/II and averages 13.40 mg/kg in Region III, while exchangeable potassium (K) varies between 72.45-136.52 mg/kg in Regions I/II and reaches 86.01 mg/kg in Region III. These zonal averages are now cross-checked with the detailed profile data. For example, in Region I (Profile 1), the humus content reaches 0.47% at a depth of 48-77 cm, which aligns with the upper range of the regional average. In Region III (Profile 5), the humus level averages around 0.26%, consistent with the summarized zonal data. Thus, all profile-based values have been re-evaluated to ensure they correspond accurately to their respective regional means. Overall, the updated results confirm that humus, phosphorus, and potassium contents are lower in the surface horizons and tend to increase in the middle layers. This pattern reflects the influence of salinity, wind-driven sand accumulation, and high temperatures characteristic of the region.

In the third region, which consists of relatively newly dried areas and is located closer to the water, specifically in the eastern part of the Aral Sea, there are five profiles with varying levels of humus and nutrient elements. In these profiles, the humus, nitrogen, phosphorus, and potassium content in the uppermost layers is lower compared to the deeper layers. This is due to higher transpiration rates, which have led to salt accumulation in the upper layers of the soils in this region.

The amount of humus (organic matter) in soil plays a key role in regulating the carbon-to-nitrogen (C:N) ratio and total nitrogen (N) concentration. Since humus itself is composed of both carbon and nitrogen, changes in its quantity directly influence soil biochemical processes. An increase in humus content generally enhances total nitrogen levels, as organic matter decomposition leads to the mineralization of nitrogen into available forms such as ammonium (NH_4^+) and nitrate (NO_3^-). The data were statistically evaluated using ANOVA for humus parameters. The results demonstrated a highly significant difference among the compared groups (Pr>T = 0.0001***), indicating that variations in humus levels significantly affect the C:N ratio and nitrogen content (Table 5). The initial interpretation describing these results as “no significant difference” appears to be inconsistent with the actual probability value ($p < 0.001$), which confirms a statistically significant effect, as shown in Table 5.

Table 5. Statistical Analysis of C:N Ratio and Nitrogen Content Across Groups (Pr>T).

Source	Value	Standard error	t	Pr > |t|	Lower bound (95%)	Upper bound (95%)	p-values signification codes
C:N	0,703	0,023	30,917	<0,0001	0,658	0,748	***
N	1,106	0,023	48,669	<0,0001	1,062	1,151	***

Signification codes: 0 < *** < 0.001 < ** < 0.01 < * < 0.05 < . < 0.1 < ° < 1

Linear Discriminant Analysis (LDA) was applied to evaluate the relationships among humus content, C:N ratio, total nitrogen (N), phosphorus (P), and potassium (K) along the studied soil profiles (Figures 10). In Figures 10-11, the results of the Linear Discriminant Analysis (LDA) reveal distinct patterns among the studied soil profiles. Profiles 1, 2, and 4 are characterized by relatively high and stable humus contents, which are closely associated with elevated total nitrogen (N) levels and well-balanced C:N ratios. In contrast, Profile 3 demonstrates lower discriminant scores, indicating reduced organic matter accumulation, whereas Profile 5 exhibits greater

dispersion along both discriminant axes, reflecting notable structural and compositional heterogeneity. These findings substantiate a statistically significant relationship between humus and nitrogen parameters. The standardized coefficients for C:N ratio and total N with respect to humus were 0.703 ± 0.023 and 1.106 ± 0.023, respectively, suggesting a strong positive correlation between humus content and nitrogen indicators. Overall, the discriminant patterns indicate that soils enriched in humus generally possess higher nitrogen availability and improved nutrient balance, while the variability observed in Profiles 3 and 5 may be attributed to differences in organic matter mineralization dynamics and humus stability.

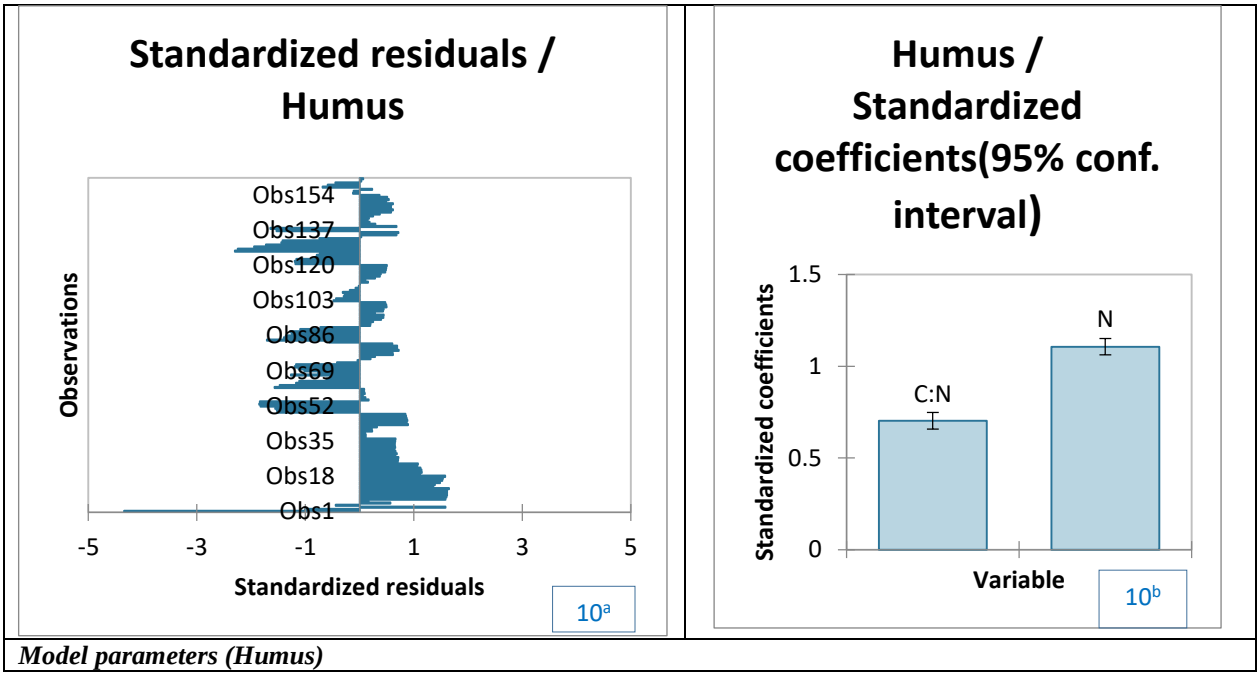

Fig. 10. The relationship between C:N and N content in soil and humus (Humus / Standardized coefficients, 95% confidence interval).

In this LDA analysis, the distribution of group samples across profiles was observed as follows when Axis 1 represented the N and C:N ratio, and Axis 2 represented humus. The distribution pattern can be seen in Figures 11.

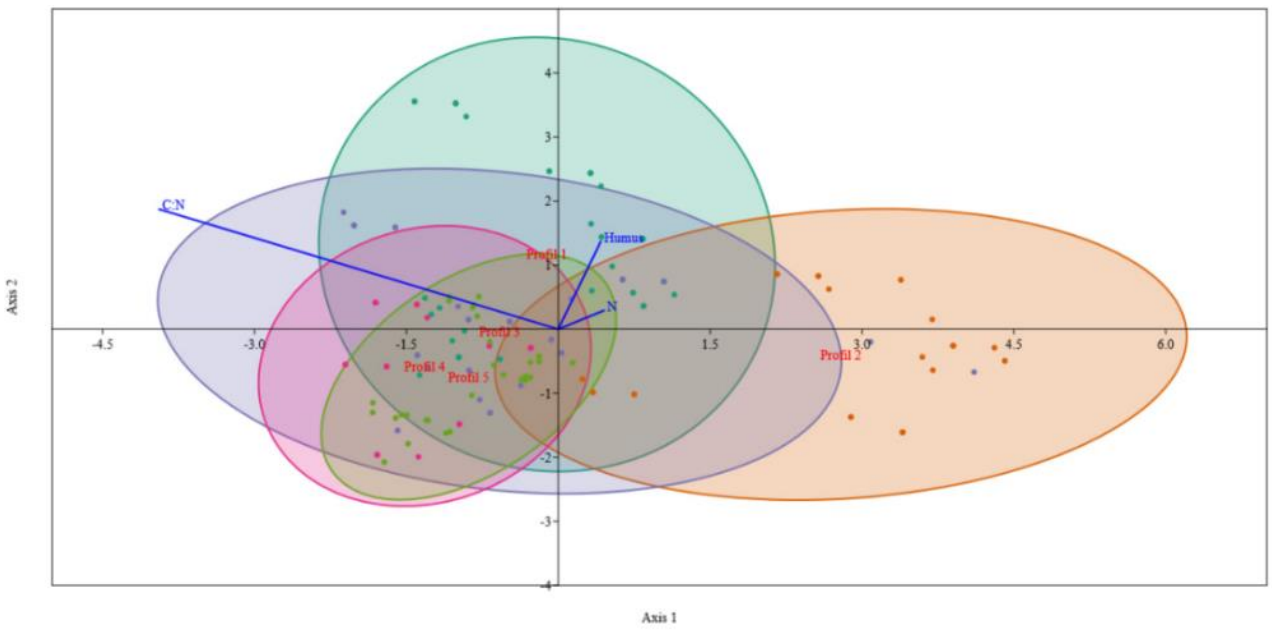

Fig. 11. Distribution of group samples according to the C:N, N indices, and Humus based on LDA (Linear Discriminant Analysis) analysis.

The ordination results demonstrate a consistent spatial alignment of samples along both axes, confirming that variations in nitrogen parameters are closely associated with humus concentration within each profile. Profiles 1 and 4 exhibit the most balanced and compact clustering, where humus and N values maintain proportional increases, suggesting more uniform organic matter decomposition and nutrient cycling. In contrast, Profiles 2 and 3 show wider dispersion, reflecting spatial heterogeneity in nitrogen mineralization rates. Profile 5 exhibits partial overlap with Profiles 1 and 4 but demonstrates weaker discriminant separation, indicating lower humus accumulation and more variable C:N ratios in deeper horizons. Overall, the LDA distribution pattern confirms a statistically coherent relationship between humus, total N, and C:N ratio across the studied profiles. This suggests that differences in organic matter composition are a major discriminating factor in soil fertility and nutrient dynamics across the regions.

3.4. Granulometric Composition of Soil

The granulometric composition of soils in the dried basin of the Aral Sea clearly reflects the ongoing transformation processes. Approximately fifty years ago, in the coastal parts of the desiccated area, the upper (0-14 cm) horizon of Profile 1 in Region I contained 18.2% particles smaller than 0.01 mm, corresponding to fine silt fractions, and exhibited a sandy texture. In the deeper layers (14-83 cm), the content of particles <0.01 mm ranged between 22% and 29.7%, forming a light-textured horizon. Below this, a more compact sand layer was observed, where the fraction of fine particles was only 7.3-8.4%. In Profile 2 of the same region, the surface layer (0-0.7 cm) consisted of loose sand with about 3% fine particles, while the 0.7-120 cm horizon had a sandy texture containing 13.8-16% fine material. In Region II, Profile 3 showed variability in fine particle content from 4% to 24.1%, indicating a gradual textural transition from loose sand to sandy loam and light sandy loam. In the central parts of the dried seabed, where 18-20 years have passed since desiccation, Profiles 4 and 5 exhibited a significant reduction in fine particle content, with the lowest value recorded at 2%. Their texture was identified as sandy. These results indicate that following the regression of the Aral Sea, the newly exposed seabed was initially covered by loose, aeolian sands with a very low proportion of fine particles. Over time, as vegetation cover began to establish and soil formation intensified under automorphic conditions that is, where the groundwater table lies deeper than 3 meters and does not influence the soil moisture regime the texture gradually evolved toward a heavier composition due to the progressive accumulation of silt and clay fractions.

The physical clay fraction (≤ 0.01 mm particles) plays an important role in soil composition as it influences the physical-chemical properties of the soil, including the content and availability of macroelements such as phosphorus (P) and potassium (K). The physical clay sum fraction increases the cation exchange capacity (CEC) of the soil, which in turn enhances the binding of phosphorus in the soil. Potassium is predominantly fixed in soil minerals such as illite and montmorillonite. The physical clay sum particles play a key role in adsorbing potassium and gradually releasing it to plants. The research results were analyzed through the Analysis of Variance (Physical clay sum) test. According to the results, no significant difference was found between the groups (Pr>F), with (0.0001***) (Table 6).

Table 6. **Analysis of Variance of P and K Content in Soil Groups (Pr>T between Groups).**

Source	Value	Standard error	t	Pr > |t|	Lower bound (95%)	Upper bound (95%)	p-values signification codes
P	0,356	0,071	5,004	<0,0001	0,216	0,497	***
K	0,370	0,071	5,196	<0,0001	0,229	0,511	***

Signification codes: 0 < *** < 0.001 < ** < 0.01 < * < 0.05 < . < 0.1 < ° < 1

The standardized residual indicators of the Physical clay sum in the research results showed that in profiles 1 and 4, 3/1 of the values were negative and the majority, 3/2, were positive. In profiles 2 and 3, 3/1 of the values were positive and the majority, 3/2, were negative. In profile 5, the majority of the values were negative (Figure 12).

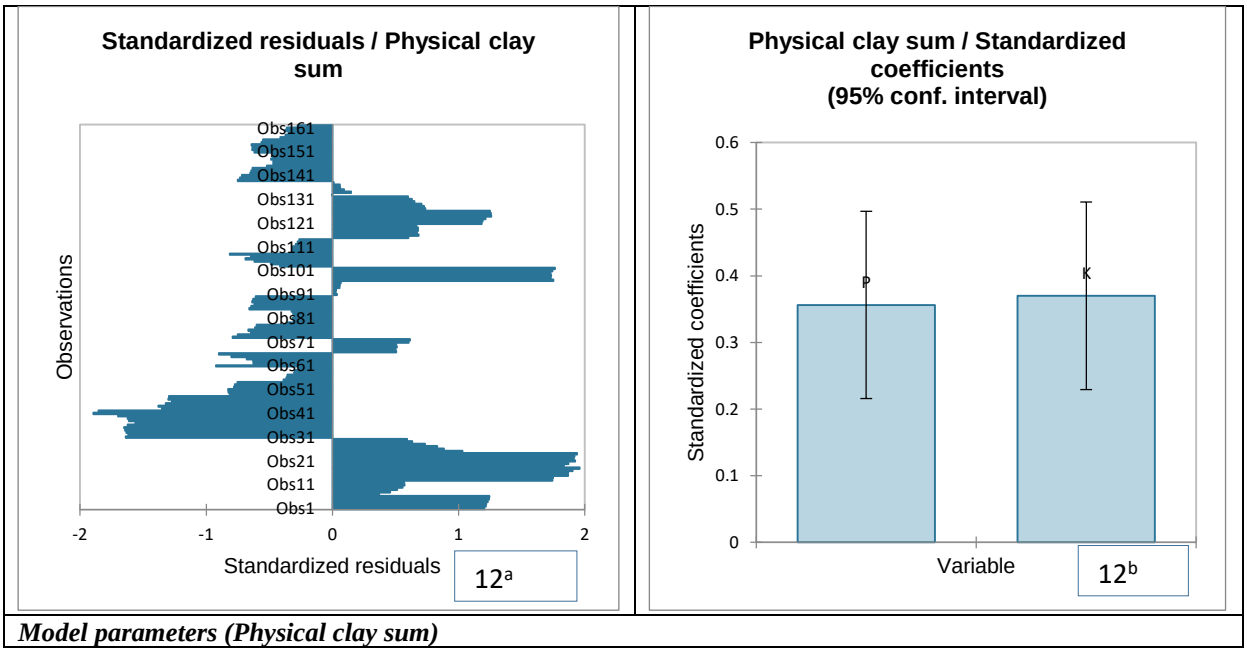

Fig. 12. The relationship between phosphorus and potassium content in soil and physical clay (Physical clay sum / Standardized coefficients, 95% conf. interval).

Figure 12 (a, b) illustrates the statistical relationship between total phosphorus (P), total potassium (K), and the physical clay fraction across the studied soil profiles. The results show that both nutrients exhibit a positive association with increasing clay content, indicating that finer soil textures contribute to higher nutrient retention. In Figure 12a, the spatial variation of P and K across the five profiles demonstrates that Profiles 1 and 3 recorded the highest nutrient concentrations, particularly within observation ranges 13-21 and 97-102, corresponding to horizons enriched with fine-grained particles. These layers, characterized by higher surface area and greater cation exchange capacity, favor the adsorption and accumulation of P and K. Profiles 2 and 4 display intermediate nutrient levels, while Profile 5 shows noticeably lower concentrations, reflecting coarser texture and possible nutrient loss through leaching or salinization processes. Figure 12b presents the standardized coefficients obtained from the regression-type model: 0.356 ± 0.071 for phosphorus (P) and 0.370 ± 0.071 for potassium (K). The similarity between these coefficients confirms that both elements respond consistently to variations in the proportion of physical clay. The narrow 95% confidence intervals indicate that the model parameters are stable and statistically reliable. Overall, the analysis of Figures 12a and 12b confirms that the physical clay fraction plays a crucial role in regulating soil nutrient dynamics. The observed increase in P and K concentrations with higher clay content highlights the importance of fine-particle composition in maintaining soil fertility and nutrient availability across the studied profiles.

Linear Discriminant Analysis (LDA) results showing the spatial distribution of total phosphorus (P) and potassium (K) in relation to the physical clay content across the five soil profiles. The LDA ordination highlights distinct clustering and separation patterns among the profiles along both discriminant axes.

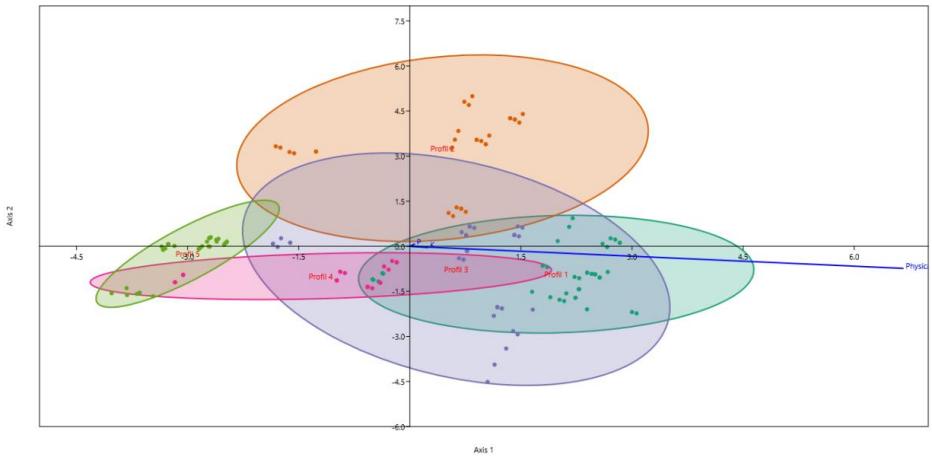

Fig. 13. Distribution of soil phosphorus and potassium indicators relative to physical clay using LDA (Linear Discriminant Analysis).

Profiles 1 and 3 exhibit similar distribution patterns along Axis 1, with profile 3 encompassing the widest range of variation across both axes, indicating stronger differentiation in nutrient behavior. Profiles 2 and 4 show partial overlap along Axis 2, reflecting moderate similarity in their P and K dynamics. In contrast, Profile 5 demonstrates reduced discriminant loading along Axis 1, suggesting lower nutrient concentrations in the deeper layers. The inverse relationship observed in Profile 5 between total P, K, and physical clay content likely results from enhanced evaporation and salt accumulation in the upper horizons, which limits nutrient mobility and retention in lower strata. Overall, the LDA results confirm that soil texture and profile depth significantly influence the spatial redistribution of phosphorus and potassium. These findings emphasize that differences in the physical composition of the soil, especially the proportion of fine particles, are key discriminating factors shaping nutrient variability across the studied sites.

4. Discussion

The findings of this research provide updated perspectives on pedogenic transformations occurring across the desiccated floor of the Aral Sea, particularly within its eastern sector. Soil formation in this region proceeds under contrasting hydromorphic (<2 m) and automorphic (>3 m) regimes. In the coastal and aeolian depositional zones, the emergence of Solonchaks in the recently exposed central area is consistent with previously described salinization and sand accumulation processes (Ismonov et al., 2024; Issanova et al., 2022). However, whereas earlier studies primarily focused on the intensity of salinity, the present results emphasize distinct variations in nutrient availability, humus accumulation, and granulometric composition among the three studied regions. These variations demonstrate that soil transformation is strongly influenced by exposure duration and geomorphological setting. According to Duan et al. (2022), the highest salt accumulation in Aralkum soils occurs within the upper 5 cm layer. Our findings confirm this observation while further revealing the downward leaching and redistribution of salts to depths of up to 120 cm, particularly in coastal profiles. This indicates that vertical salt dynamics are more complex than previously assumed, being regulated by episodic moisture inputs and aeolian redistribution.

The relatively higher humus content observed in Regions I and II contrasts with the extremely low organic matter levels reported by Kim et al. (2024) for recently formed soils on the Aral seabed. Such differences are attributed to longer exposure periods and partial stabilization of halophytic shrubs in the coastal and aeolian-affected areas, which enhance organic matter input. Conversely, the very low humus content in the central Solonchaks corresponds to their more recent desiccation history and elevated salinity, both of which limit vegetation establishment (Šimonovičová et al., 2024). Granulometric analysis supports the interpretation proposed by Stulina et al. (2020), who noted that the southeastern Aral Basin is dominated by carbonate-rich sandy and silty deposits. The current study reveals a progressive increase in fine-textured (clay-sized) fractions from the coastal region toward the central zone, indicating a gradual refinement of soil texture. This trend suggests potential improvement in cation exchange capacity and nutrient retention over time. Nonetheless, the pronounced spatial heterogeneity in particle-size distribution highlights the governing influence of local depositional and aeolian processes on soil texture and composition. Although salinization remains the principal constraint on soil genesis, the combined effects of exposure duration, vegetation development, and granulometric differentiation are fostering a clear distinction between Arenosols and Solonchaks. These findings are consistent with the conceptual framework proposed by Jabbarov et al. (2025), which posits that soil development on the Aral seabed follows a mosaic and non-linear trajectory governed by site-specific environmental conditions.

In conclusion, this study underscores the necessity of accounting for spatial heterogeneity in soil transformation processes when designing regionally adapted management and reclamation strategies for the Aral Sea Basin.

5. Conclusions

The drying of the Aral Sea is considered the third drying event in its evolutionary history. Over several hundred thousand years, the filling and drying of the water led to the formation of soils in its place, and this process continues to this day. These soils undergo transformation due to climate change and the passage of time. To study soil transformation, the area was divided into Regions I, II, and III for comparison. The results showed that the transformation process occurred most rapidly along the coasts of the Aral Sea, where it had initially dried. In Regions I and II, Arenosols formed, while in Region III, Solonchaks developed. The study also revealed that the amounts of humus, nitrogen, phosphorus, and potassium were higher in the profiles of Regions I and II, while in Region III, their appearance was slower and their quantities lower. The amount of salts was also lower in the soils of Regions I and II, whereas higher salt concentrations and the formation of salinized soils were observed in Region III. The types of salinization were chloride, sulfate-chloride, and chloride-sulfate. In conclusion, the formation and transformation of soils in the dried-up bottom of the Aral Sea do not follow a consistent pattern. The distribution of salts is varied, as the salts did not originate from the parent materials of the soils but were primarily derived from the composition of the Aral Sea's water. As the water disappeared, salts accumulated in

both the surface and subsurface layers of the land and spread to surrounding areas due to wind influence. Over time, a pattern of soil transformation may emerge, leading to the development of distinct soil layers.

Declarations

Ethics approval and consent to participate

Consent for publication: The article does not contain any material that is unlawful, defamatory, or would in any way violate the terms and conditions set forth in the contract if published.

Availability of data and material: Not applicable.

Competing interests: The authors declare that there is no conflict of interest in the publication.

Funding Statement: This article was carried out as part of the project financed by the Innovation Development Agency of the Republic of Uzbekistan under the project number FL-8323102111, titled “Creating a scientific basis for grouping areas for planting plants according to the salinity, physical, chemical, and biological properties of the soils distributed in the dry bottom of the Aral Sea.

Authors' contributions: Authors ZJ, TA, KhE, UN, ShA wrote the original draft and EY, DM, OI, NZ, BW, SS edit and finalize the manuscript. All authors read and agree for submission of the manuscript to the journal.

Acknowledgments: The authors express their gratitude to the Agency for Innovative Development of the Republic of Uzbekistan and the leadership of the Faculty of Biology, who funded this research under the FL-8323102111 project.

Resferences

Alikhanova, S., & Bull, J. W. (2023). Review of nature-based solutions in dryland ecosystems: The Aral Sea case study. Environmental Management, 72(3), 457-472. https://doi.org/10.1007/s00267-023-01822-z

Aslanov, I., Teshaev, N., Jabbarov, Z., Opp, C., Oymatov, R., Karimov, Y., & Henebry, G. (2024). Characterizing land surface dynamics in Aral Sea basin of Uzbekistan using climatic and remote sensing data to project future conditions. E3S Web of Conferences, 575, 04009. https://doi.org/10.1051/e3sconf/202457504009

Aslanov, I., Teshaev, N., Jabbarov, Z., Opp, C., Oymatov, R., Karimov, Y., & Henebry, G. (2024). Characterizing land surface dynamics in Aral Sea basin of Uzbekistan using climatic and remote sensing data to project future conditions. E3S Web of Conferences, 575, 04009. https://doi.org/10.1051/e3sconf/202457504009

Aus der Beek, T., Voß, F., & Flörke, M. (2011). Modelling the impact of global change on the hydrological system of the Aral Sea basin. Physics and Chemistry of the Earth, 36(13), 684-695. https://doi.org/10.1016/j.pce.2011.03.004

Badescu, V., & Schuiling, R. D. (2010). Aral Sea: Irretrievable loss or Irtysh imports?. Water Resources Management, 24(3), 597-616. https://doi.org/10.1007/s11269-009-9461-y

Berdimbetov, T., Ilyas, S., Ma, Z., Bilal, M., & Nietullaeva, S. (2021). Climatic change and human activities link to vegetation dynamics in the Aral Sea basin using NDVI. Earth Systems and Environment, 5, 303-318. https://doi.org/10.1007/s41748-021-00224-7

Berdimbetov, T., Pushpawela, B., Murzintcev, N., Nietullaeva, S., Gafforov, K., Tureniyazova, A., & Madetov, D. (2024). Unraveling the intricate links between the dwindling Aral Sea and climate variability during 2002-2017. Climate, 12(7), 105. https://doi.org/10.3390/cli12070105

Breckle, S. W., & Geldyeva, G. V. (2012). Dynamics of the Aral Sea in geological and historical times. In S. W. Breckle, W. Wucherer, L. Dimeyeva, & N. Ogar (Eds.), Aralkum - a man-made desert. Ecological Studies (Vol. 218, pp. 23-42). Springer. https://doi.org/10.1007/978-3-642-21117-1_2

Christian, O., Michael, G., Oleg, S., Natalya, V., & Asia, K. (2019). Impact of the Aral Sea syndrome - The Aralkum as a man-made dust source. [Conference presentation].

Cretaux, J.-F., Letolle, R., & Bergé-Nguyen, M. (2013). History of Aral Sea level variability and current scientific debates. Global and Planetary Change, 110, 99-113. https://doi.org/10.1016/j.gloplacha.2013.05.006

Duan, Z., Wang, X., & Sun, L. (2022). Monitoring and mapping of soil salinity on the exposed seabed of the Aral Sea, Central Asia. Water, 14(9), 1438. https://doi.org/10.3390/w14091438

Duan, Z., Wang, X., & Sun, L. (2022). Monitoring and mapping of soil salinity on the exposed seabed of the Aral Sea, Central Asia. Water, 14(9), 1438. https://doi.org/10.3390/w14091438

He, H., Hamdi, R., Luo, G., et al. (2022). The summer cooling effect under the projected restoration of Aral Sea in Central Asia. Climatic Change, 174, 13. https://doi.org/10.1007/s10584-022-03434-8

Huang, S., Chen, X., Chang, C., Liu, T., Huang, Y., Zan, C., Ma, X., De Maeyer, P., & Van de Voorde, T. (2022). Impacts of climate change and evapotranspiration on shrinkage of the Aral Sea. Science of the Total Environment, 845, 157203. https://doi.org/10.1016/j.scitotenv.2022.157203

Indoitu, R., Kozhoridze, G., Batyrbaeva, M., Vitkovskaya, I., Orlovsky, N., Blumberg, D., & Orlovsky, L. (2015). Dust emission and environmental changes in the dried bottom of the Aral Sea. Aeolian Research, 17, 101-115.

https://doi.org/10.1016/j.aeolia.2015.02.004

Indoitu, R., Kozhoridze, G., Batyrbaeva, M., Vitkovskaya, I., Orlovsky, N., Blumberg, D., & Orlovsky, L. (2015). Dust emission and environmental changes in the dried bottom of the Aral Sea. Aeolian Research, 17, 101-115. https://doi.org/10.1016/j.aeolia.2015.02.004

Ismonov, A., Dusaliev, A., Kalandarov, N., Mamajanova, U., & Kattaeva, G. (2024). Profile of desert sandy soils formed in the Aral Sea dried-up seabed. E3S Web of Conferences, 486, 04010. https://doi.org/10.1051/e3sconf/202448604010

Issanova, G., Abuduwaili, J., & Tynybayeva, K. (2023). Environmental conditions of the Aral Sea region. In Soil cover of the dried Aral seabed in Kazakhstan (pp. 25-44). Springer. https://doi.org/10.1007/978-3-031-29867-7_2

Issanova, G., Abuduwaili, J., Tynybayeva, K., et al. (2022). Assessment of the soil cover in the dried Aral seabed in Kazakhstan and climate change in the region. Water, Air, & Soil Pollution, 233, 525. https://doi.org/10.1007/s11270-022-05966-2

IUSS Working Group WRB. (2022). World Reference Base for Soil Resources, 2022: International soil classification system for naming soils and creating legends for soil maps (4th edition). International Union of Soil Sciences (IUSS), Vienna, Austria.

Izhitskiy, A., Zavialov, P., Sapozhnikov, P., et al. (2016). Present state of the Aral Sea: Diverging physical and biological characteristics of the residual basins. Scientific Reports, 6, 23906. https://doi.org/10.1038/srep23906

Jabbarov, Z., Abdrakhmanov, T., Zakirova, S., Abdushukurova, Z., Sultanova, N., Abdullaev, Sh., Matkarimova, A., Nomozov, U., Musurmanov, A., Kaxorov, B., Berdiev, T. (2024). Post-Reclamation Enhancement of Physical and Biological Properties of Soils Contaminated by Oil and Petroleum Products. E3S Web of Conferences 590, 01003. https://doi.org/10.1051/e3sconf/202459001003

Jabbarov, Z., Abdrakhmanov, T., Tashkuziev, M., Abdurakhmonov, N., Makhammadiev, S., Fayzullaev, O., Nomozov, U., Kenjaev, Y., Abdullaev, S., Yagmurova, D., Abdushukurova, Z., Iskhakova, S., & Kováčik, P. (2024). Cultivation of plants based on new technologies in the dry soil of the Aral Sea. E3S Web of Conferences, 497, 03008. https://doi.org/10.1051/e3sconf/202449703008

Jabbarov, Z., Kholdorov, Sh., Nomozov, Makhammadiev, S., Djalilova, G,. Abdullaev, Sh,. (2025). The drying of the Aral Sea: Soil formation and restoration potential on the seabed. Soil Sci. Ann., 76(2)207727. https://doi.org/10.37501/soilsa/207727

Jabbarov, Z., Abdrakhmanov, T., Abdullaev, Sh., Makhammadiev, S., Nomozov, U., Rakhmatullaeva, G., Kovácik, P. (2025). Evaluation of carbonate accumulation, inorganic carbon content, and soil property changes in newly developed soils of degraded landscapes. Published in Journal of Degraded and Mining Lands Management. 12, no. 4. https://doi.org/10.15243/jdmlm.2025.124.7993

Jiang, L., Jiapaer, G., Bao, A., Yuan, Y., Zheng, G., Guo, H., Yu, T., & De Maeyer, P. (2020). The effects of water stress on croplands in the Aral Sea basin. Journal of Cleaner Production, 254, 120114. https://doi.org/10.1016/j.jclepro.2020.120114

Kattaeva, G. N., & Ismonov, A. Zh. (2022). Solonchars formed on the dry bottom of the Aral Sea. Научное обозрение, 4, 112-118.

Khaydar, D., Chen, X., Huang, Y., Ilkhom, M., Liu, T., Friday, O., Farkhod, A., Khusen, G., & Gulkaiyr, O. (2021). Investigation of crop evapotranspiration and irrigation water requirement in the lower Amu Darya River Basin, Central Asia. Journal of Arid Land, 13(1), 23-39. https://doi.org/10.1007/s40333-021-0054-9

Kim, G., Ahn, J., Chang, H., An, J., Khamzina, A., Kim, G., & Son, Y. (2024). Effect of vegetation introduction versus natural recovery on topsoil properties in the dried Aral Sea bed. Land Degradation & Development, 35(13), 3935-4160. https://doi.org/10.1002/ldr.5209

Loodin, N. (2020). Aral Sea: An environmental disaster in twentieth century in Central Asia. Modeling Earth Systems and Environment, 6(4), 2495-2503. https://doi.org/10.1007/s40808-020-00837-3

Micklin, P. (2007). The Aral Sea disaster. Annual Review of Earth and Planetary Sciences, 35(1), 47-72. https://doi.org/10.1146/annurev.earth.35.031306.140120

Micklin, P. (2010). The past, present, and future Aral Sea. Lakes & Reservoirs: Science, Policy and Management for Sustainable Use, 15(3), 193-213. https://doi.org/10.1111/j.1440-1770.2010.00437.x

Micklin, P. (2016). The future Aral Sea: Hope and despair. Environmental Earth Sciences, 75, 844. https://doi.org/10.1007/s12665-016-5614-5

Micklin, P. P., & Williams, W. D. (2019). The Aral Sea Basin. Routledge. https://doi.org/10.4324/9780429436475

Micklin, P., & Aladin, N. V. (2008). The Aral Sea. Scientific American, 298(4), 64-71. https://doi.org/10.1038/scientificamerican0408-64

Opp, C., Groll, M., Semenov, O., Shardakova, L., Kovalevskaya, Y., Kulmatov, R., Normatov, I., & Aslanov, I. (2024). Water household changes, climate change, and human impact - Reasons for the dusty side of the Aral Sea syndrome. E3S

Web of Conferences, 575, 04001. https://doi.org/10.1051/e3sconf/202457504001

Orlovsky, N., Glantz, M., & Orlovsky, L. (2001). Irrigation and land degradation in the Aral Sea basin. In S. W. Breckle, M. Veste, & W. Wucherer (Eds.), Sustainable land use in deserts (pp. 173-190). Springer. https://doi.org/10.1007/978-3-642-59560-8_11

Peter, Z. (2005). Physical oceanography of the dying Aral Sea. Springer. https://doi.org/10.1007/b138791

Rufin, P., et al. (2022). Post-Soviet changes in cropping practices in the irrigated drylands of the Aral Sea basin. Environmental Research Letters, 17(9), 095013. https://doi.org/10.1088/1748-9326/ac8daa

Šimonovičová, A., Pauditšová, E., Nosalj, S., Oteuliev, M., Klištincová, N., Maisto, F., Kraková, L., Pavlović, J., Šoltys, K., & Pangallo, D. (2024). Fungal and prokaryotic communities in soil samples of the Aral Sea dry bottom in Uzbekistan. Soil Systems, 8(2), 58. https://doi.org/10.3390/soilsystems8020058

Stulina, G. V., Kharitonova, G. V., Krutikova, V. O., Shein, E. V., & Berdnikov, N. V. (2020). Carbonates in the soils of the Aral Sea dried bottom. IOP Conference Series: Materials Science and Engineering, 941(1), 012017. https://doi.org/10.1088/1757-899X/941/1/012017

Su, Y., Li, X., Feng, M., Nian, Y., Huang, L., Xie, T., Zhang, K., Chen, F., Huang, W., Chen, J., & Chen, F. (2021). Science of the Total Environment, 777, 145993. https://doi.org/10.1016/j.scitotenv.2021.145993

Waltham, T., & Sholji, I. (2001). The demise of the Aral Sea - an environmental disaster. Geology Today, 17(6), 218-228. https://doi.org/10.1046/j.0266-6979.2001.00319.x

Zonn, I. S., Glantz, M. H., Kostianoy, A. G., & Kosarev, A. N. (2009). The Aral Sea encyclopedia. Springer.

GOST 12536. (2014). Soils. Methods for Laboratory Determination of Grain-Size and Microaggregate Composition. Interstate Council for Standardization, Metrology and Certification (EASC), Moscow, Russia.

GOST 26213-91. (1991). Soils. Determination of Organic Matter and Organic Carbon by the Dichromate Oxidation Method. Interstate Council for Standardization, Metrology and Certification (EASC), Moscow, Russia.

GOST 26107-84. (1984). Soils. Determination of Total Nitrogen by the Kjeldahl Method. Interstate Council for Standardization, Metrology and Certification (EASC), Moscow, Russia.

GOST 26205-91. (1991). Soils. Determination of Mobile and Total Phosphorus by Extraction with Ammonium-Lactate Solution. Interstate Council for Standardization, Metrology and Certification (EASC), Moscow, Russia.

GOST 26204-91. (1991). Soils. Determination of Exchangeable and Total Potassium by Flame Photometry. Interstate Council for Standardization, Metrology and Certification (EASC), Moscow, Russia.

Dukhovny, V. A. (Ed.). (2017). The Aral Sea and the Aral Region. Tashkent: Baktria Press.

Idirisov, K. A., Bobomuratov, Sh. M., & Mirzambetov, A. B. (2023). Soil-reclamation state of the southeastern part of the dried bottom of the Aral Sea. Soil Science and Agrochemistry, 4.